Pulmonary benign ground-glass nodules: CT features and pathological findings

Wang-jia Li
The First Affiliated Hospital of Chongqing Medical University
Fa-jin Lv
The First Affiliated Hospital of Chongqing Medical University
Yi-wen Tan
The First Affiliated Hospital of Chongqing Medical University
Bin-jie Fu
The First Affiliated Hospital of Chongqing Medical University
Zhigang Chu (chuzg0815@163.com)
Chongqing Medical University First Affiliated Hospital https://orcid.org/0000-0002-2441-8132

Research article

Keywords: ground-glass nodule, benign, CT, pathology, lung

Posted Date: October 23rd, 2020

DOI: https://doi.org/10.21203/rs.3.rs-93907/v1

Abstract

Background: Some pulmonary ground-glass nodules (GGNs) are benign and frequently misdiagnosed due to lack of understanding of their CT characteristics. This study aimed to reveal the CT features and corresponding pathological findings of pulmonary benign GGNs to help improve diagnostic accuracy.

Methods: From March 2016 to October 2019, patients with benign GGNs confirmed by operation or follow-up were enrolled retrospectively. According to overall CT manifestations, GGNs were classified into three types: I, GGO with internal high-attenuation zone; II, nodules lying on adjacent blood vessels; and other type, lesions without obvious common characteristics. CT features and pathological findings of each nodule type were evaluated.

Results: Among the 40 type I, 25 type II, and 14 other type GGNs, 24, 19, and 10 nodules were resected, respectively. Type I GGNs were usually irregular with only one high-attenuation zone (main pathological components: thickened alveolar walls with inflammatory cells, fibrous tissue, and exudation), which was usually centric, having blurred margin, and connecting to blood vessels. The peripheral GGO (main pathological component: a small amount of inflammatory cell infiltration with fibrous tissue proliferation) was usually ill-defined. Type II GGNs (main pathological components: focal interstitial fibrosis with or without inflammatory cells infiltration) lying on adjacent vessel branches were usually irregular and well-defined, but showed coarse margins. Other type GGNs had various CT manifestations but their pathological findings were similar to that of type II.

Conclusion: For subsolid nodules with CT features manifested in type I or II GGNs, follow-up should be firstly considered in further management.

Background

The advent of CT screening for lung cancer has increased the incidence of ground-glass nodules (GGNs). GGNs, especially part-solid GGNs, are more likely to be lung cancer than solid nodules [1–4]. Furthermore, most part-solid GGNs are confirmed as minimally invasive adenocarcinomas or invasive adenocarcinomas, often requiring surgical resection [5, 6]. Although GGNs have a high probability of malignancy, quite a few lesions were benign. Among them, most are transient and a small number of persistent lesions are finally confirmed as focal interstitial fibrosis [7–9]. These GGNs are often misdiagnosed as lung cancers and treated by unnecessary surgical resection. Therefore, carefully discriminating benign GGNs from malignant ones remains a challenge.

Previous studies have investigated the differences in CT features between benign and malignant GGNs, and found that larger size, lobulation, spiculation, air bronchogram, and solid component were indicative of malignancy [10–13]. However, Felix et al. [14] found that the resolving GGNs were more likely to be lobular, polygonal, mixed, and larger than persistent GGNs, which was contrary to the results of other studies. Additionally, these studies only revealed the relative CT features of benign GGNs but failed to summarize their common CT characteristics, resulting in limited differential diagnostic value. Therefore,

further studies should focus on determining whether benign GGNs have some distinct features to help improve diagnostic accuracy of benign GGNs.

In clinical practice, we found that benign GGNs had various CT manifestations, but some of them had similar CT features, which were not well studied. We hypothesize that benign GGNs have some relatively consistent CT characteristics. In this study, benign GGNs were classified into different types based on overall manifestations and CT features of each nodule type were further investigated and summarized. Furthermore, their pathological findings were also studied. These results may provide additional information for understanding benign GGNs and differentiating between benign and malignant nodules.

Methods

This retrospective study used non-identifiable data and have no potential risks to patients, so the institutional review board approved this study and waived the requirement for informed consent.

Patients

From March 2016 to October 2019, patients with surgically resected and pathologically confirmed benign GGNs or GGNs resolved during follow-up were enrolled retrospectively. Inclusion criteria were as follows: (1) the lesion was a GGN (diameter, ≤ 3 cm); (2) availability of thin-section CT images with a thickness ≤ 1 mm; (3) the patients' clinical and pathological data were complete for those with resected GGNs. Exclusion criteria were as follows: (1) patients with diffused lesions, which would influence the evaluation; and (2) CT images contained significant motion artifacts. Finally, 79 patients with benign GGNs were enrolled in this study. The patient selection procedure was shown in Fig 1.

CT examinations

All patients were scanned on a 128-slice MDCT scanner (SOMATOM Definition Flash system, Siemens Medical Systems) at the end of inspiration during a single breath-hold. Non-contrast CT examinations were performed with the following parameters: tube voltage, 110–120 kV; tube current, 50–150 mAs; beam pitch, 1.0; detector collimation, 0.6 mm; rotation time, 0.5 s. All patients were scanned from the thoracic inlet to the lung base using 5 mm section thickness and 5 mm section spacing. The data were reconstructed into the images with slice thickness ≤ 1 mm using a high-resolution reconstruction kernel and displayed with a standard lung window setting (width, 1600 HU; level, −600 HU).

CT data analysis

All patients' CT data were independently reviewed on a PACS workstation (Carestream Vue PACS) by 2 radiologists (Z.G.C. and F.J.L.) with more than 10 years' experience of chest CT interpretation who were blinded to the pathological results of nodules. Data analysis was performed on both the original and reformatted images.

Based on the overall CT manifestations of nodules, GGNs were classified into three types: type I: ground-glass opacity (GGO) with internal high-attenuation zone (Fig. 2A); Type II: GGNs lying on adjacent blood vessels (Fig. 2B); Other type: GGNs with other various CT features rather than those manifested in type I and II nodules. Type II and other type GGNs had no significant solid component. The following CT features were further evaluated for each GGN type: nodule location, shape (round/oval or irregular), diameter (mean of the longest diameter and perpendicular diameter on axial images), border (well-defined or ill-defined), and margin of well-defined lesion (smooth or coarse). Additionally, for type I GGNs, the number, location, shape, diameter, and edge (clear or blurred) of high-attenuation zone, whether the high-attenuation zone connected to blood vessels (artery or vein), and the uniformity of peripheral GGO component (homogeneous or heterogeneous) were assessed. For type II GGNs, the uniformity of nodules and the adjacent blood vessels (artery or vein; normal, dilated, or distorted) lied by nodules were evaluated. When the interpretations of two radiologists differed, the divergences were resolved by consensus.

Statistical analysis

All statistical analyses were performed using the Statistical Package for Social Sciences program (version 22.0, IBM, Armonk, NY). Continuous data are presented as mean ± standard deviation, while categorical data are presented as numbers and percentages. Statistical differences of three GGN types were analyzed using the Wilcoxon rank sum test for patient age, WBC and eosinophil count, and mean diameter of GGN. And patient's sex, smoking and drinking history, mode of detection, and CT characteristics (lesion location, shape, border, and margin of well-defined nodules) were analyzed using the Pearson x^2 test and Fisher exact test, as appropriate. A P value < .05 indicated a significant difference.

Results

Patients' clinical characteristics

Seventy-nine patients (mean age: 53 ± 11 years; range: 19–79 years) were included, comprising 32 (40.5%) men (mean age: 55 ± 10.5 years; range: 36–79 years) and 47 (59.5%) women (mean age: 51 ± 11 years; range: 19–68 years). Among 79 patients with GGNs, 53 (67.1%) were confirmed by surgical resection and pathological examination, and 26 (32.9%) by disappearance during follow-up (mean follow-up time: 4.8 months ± 4.5; range: 0.5 ~ 16 months). A total of 24 resected GGNs had follow-up results (mean follow-up time: 3.0 months ± 2.9; range: 0.3 ~ 8.5 months), 22 (91.7%) GGNs had no significant change, and 2 (8.3%) GGNs showed a slight decrease in size or density. At 3 months after first detection, most of transient GGNs (19/26, 73.1%) resolved, whereas most of resected nodules (22/24, 91.7%) remained stable.

Among 79 patients, there were 40 (50.6%), 25 (31.6%), and 14 (17.7%) patients with type I, type II, and other type GGNs, respectively. There were more women (P = .041), nonsmokers (P = .003) and nondrinkers (P = .003) in type II than in other two types. Eosinophil count was higher in patients with type I GGNs than

that in patients with type II and other type lesions ($P < .001$), and eosinophilia was observed in 3 patients with type I GGNs. Patients' clinical characteristics are summarized in Table 1.

Table 1
Clinical features of patients with different types of benign GGNs

Clinical features	Type I (n = 40)	Type II (n = 25)	Other type (n = 14)	P value
Sex				
Man	20 (50.0)	5 (20.0)	7 (50.0)	.041‡
Woman	20 (50.0)	20 (80.0)	7 (50.0)	
Age (y)	53 ± 11	54 ± 11	50 ± 10	.838&
Current or former smoker	18 (45.0)	2 (8.0)	6 (42.9)	.003§
Current or former drinker	16 (40.0)	1 (4.0)	3 (21.4)	.003§
Surgically resected	24 (60.0)	19 (76.0)	10 (71.4)	-
Resolved in follow-up	16 (40.0)	6 (24.0)	4 (28.6)	-
Follow-up time (month)*	4.5 ± 4.4	2.4 ± 0.5	7.4 ± 5.4	-
Mode of detections				
Accidentally found	4 (10.0)	4 (16.0)	3 (21.4)	
Found by physical examination	29 (72.5)	14 (56.0)	10 (71.4)	.413§
Symptomatically found	7 (17.5)	7 (28.0)	1 (7.1)	
Malignancy history	2 (5.0)	1 (4.0)	1 (7.1)	-
WBC (uL^{-1})	6872 ± 2931	6131 ± 2900	6087 ± 1733	.296&
Eosinophil (uL^{-1})	154 ± 223	94 ± 100	70 ± 38	.001&

Data are presented as n (%) or Means ± standard deviation.

*Data are collected from patients with resolved GGNs.

‡Calculated with the Pearson χ^2 test.

§Calculated with the Fisher's exact test.

&Wilcoxon rank sum test.

CT features of different types of benign GGNs

CT features of each GGN type are summarized in Table 2. There were no significant differences in their location, diameter, shape, and margin of well-defined nodules among different types (P = .384, p = .299, P = .527, and P = .540, respectively), whereas there was a significant difference in lesion border (P = .010). Benign GGNs were mainly located in the upper lobes and had irregular shape. Type II and other type GGNs were usually well-defined but had coarse margins. For each type of benign GGNs, there were no significant differences in their CT features between resolving and resected ones, except for the diameter in type II (P = .006).

Table 2
Thin-section CT features of different types of benign GGNs

CT features	Type I (n = 40)	Type II (n = 25)	Other types (n = 14)	*P* value
Lesion location				
Right upper lobe	15 (37.5)	13 (52.0)	6 (42.9)	.384§
Right middle lobe	2 (5.0)	2 (8.0)	4 (28.6)	
Right lower lobe	7 (17.5)	4 (16.0)	1 (7.1)	
Left upper lobe	11 (27.5)	4 (16.0)	3 (21.4)	
Left lower lobe	5 (12.5)	2 (8.0)	0 (0.0)	
Mean diameter (mm)	11.4 ± 4.8	9.2 ± 3.3	9.8 ± 2.9	.299&
Uniformity of GGO or GGN				
Homogeneous	18 (45.0)	12 (48.0)	4 (28.6)	-
Heterogenous	22 (55.0)	13 (52.0)	10 (71.4)	
Lesion shape				
Round/oval	15 (37.5)	6 (24.0)	4 (28.6)	.527§
Irregular	25 (62.5)	19 (76.0)	10 (71.4)	
Lesion border				
Ill-defined	28 (70.0)	9 (36.0)	5 (35.7)	.010‡
Well-defined	12 (30.0)	16 (64.0)	9 (64.3)	
Margin of well-defined nodules				
Coarse	11 (91.7)	15 (93.8)	7 (77.8)	.540§
Smooth	1 (8.3)	1 (6.3)	2 (22.2)	

Note. Data are presented as n (%) or Means ± standard deviation.

‡Calculated with the Pearson χ^2 test.

§Calculated with the Fisher's exact test.

&Wilcoxon rank sum test.

For type I GGNs, the peripheral GGO components were frequently ill-defined (28/40, 70.0%). Most of nodules (38/40, 95.0%) only had a single high-attenuation zone with a mean diameter of 3.5 mm (range:

1.2 ~ 7.5 mm). Among the 40 high-attenuation zones, 24 (60.0%) were centric and 16 (40.0%) were eccentric, 22 (55.0%) were regular (round or oval) and 18 (45.0%) were irregular, 38 (95.0%) had blurred edge and 2 (5.0%) had clear edge, and 32 (80.0%) connected to adjacent blood vessels (arteries: 20/32, 62.5%, veins: 12/32, 37.5%) (Fig. 3, Fig. 4).

For 25 type II GGNs, 14 (56.0%) abutted the pulmonary artery branches and 11 (44.0%) abutted the pulmonary vein branches, but these vessels had no significant changes in morphology (Fig. 5, Fig. 6). In addition, 12 (48.0%) and 13 (52.0%) cases were homogeneous and heterogeneous, respectively.

Fourteen other type GGNs included 5 (35.7%) lesions with bubble lucency, 4 (28.6%) clinging to pleura or fissure with wide base, 3 (21.4%) with faint density and ill-defined border, and 2 (14.3%) with significant irregular shape.

Pathological findings

The pathological findings of 53 surgically resected GGNs were reviewed. In 24 type I GGNs, the pathological components were thickened alveolar walls with inflammatory cells, fibrous tissue and exudation (22, 91.7%) and granuloma (2, 8.3%) for internal high-attenuation zones, and a small amount of inflammatory cell infiltration with (21, 87.5%) and without (3, 12.5%) fibrous tissue proliferation for peripheral GGOs. The main pathological findings were similar for 19 type II and 10 other type GGNs, including focal interstitial fibrosis (type II GGNs: 8/19, 42.1%; other type GGNs: 4/10, 40.0%) and fibrous tissue proliferation with inflammatory cell infiltration (type II GGNs: 11/19, 57.9%; other type GGNs: 6/10, 60.0%).

Discussion

Pulmonary GGNs have a high probability of being malignant, but some of them are benign, frequently misdiagnosed as lung cancers and treated by unnecessary surgical resection. Thus, being able to recognize benign GGNs by CT is important. Previous studies failed to summarize the common features predictive of benign GGNs [15, 16]. In this study, we investigated benign GGNs and found that they had some common CT features, which could be explained well by their pathological findings. These new findings may be helpful for distinguishing the potential benign GGNs.

Among benign GGNs, type I lesions were the most common. Their internal high-attenuation zones were mostly single, usually having blurred edge and connecting to the adjacent blood vessels. And the peripheral GGOs were usually ill-defined, which was consistent with a previous study [17]. Pathologically, the high-attenuation zone within GGN represents the inflammation and exudation, which lead to its blurred edge. In addition, inflammation in high-attenuation zone were more severe than those in the peripheral GGO area. This indicate that the high-attenuation zone may be the primary lesion originating from terminal bronchioles, while the peripheral GGO was just caused by it.

Oh et al. [18] reported that transient GGN, especially transient part-solid GGN, might result from eosinophil infiltration and blood eosinophil count was expected to be an indicator of lesion benignity or malignancy. However, blood eosinophilia showed very low sensitivity [19]. In this study, only 3 patients with type I GGNs had eosinophilia. Thus, pulmonary eosinophil infiltration might be responsible for a very small portion of benign part-solid GGNs.

The most noteworthy feature of type II GGNs was that lesions abutted adjacent blood vessels but did not surround and affect them. This manifestation may be related to the peripheral interstitium of blood vessels, which possibly act as a barrier to inflammatory extension [20]. To determine the relationship between nodules and blood vessels, multiplanar reconstruction (MPR) is a basic tool. When a blood vessel is close to the edge of a GGN or a GGN locates at a vessel bifurcation on axial images, MPR is essential for evaluating the relationship between lesions and blood vessels.

It is worth mentioning that part-solid GGNs are also frequently detected in malignancy. However, in our experience, and those from the literature, solid components in malignant GGNs are often irregular and have coarse margins or present as multiple spots [21], and the peripheral GGOs are usually well-defined. In contrast to type II benign GGNs, malignant GGNs tended to wrap and drag vessels into lesions [22]. Gao et al [22] and Lv et al [23] found that the blood vessels passing through the nodules without any changes were commonly observed in both benign and malignant GGNs, but distorted and/or dilated vessels were more frequently observed in malignant GGNs. These differences could help to differentiate benign and malignant GGNs.

Most benign GGNs could resolve during follow-up, but a few persist. The guidelines of British Thoracic Society and the Fleischner Society recommend an initial follow-up CT scan 3 months after first detection [24, 25], which is an appropriate interval to wait before determining the possible intervention [26, 27]. In this study, the mean resolved time of transient GGNs was 4.8 months and most GGNs disappeared within 3 months, which was consistent with a previous report [18]. However, most of the resected nodules with follow-up CT remained stable at 3 months. This difference may be related to different pathological components. Therefore, although some nodules with these certain features had no change at 3 months, follow-up was still recommended.

There are several limitations in this study. First, the benign GGNs were confirmed by operation or follow-up. Although GGNs were confirmed as benignity through different ways, this brings us more knowledge. For the nodules with similar manifestations, some could provide information about their pathological components and others indicate whether they would resolve in the future. Second, it was unknown whether CT features presented in type I and II GGNs could be found in malignant GGNs. This study primarily aimed to find those nodules requiring follow-up after first detection by identifying the common CT features of benign GGNs, but not to determine their unique characteristics. Our next study will be comparing the benign and malignant GGNs with similar CT features, such as the part-solid nodules. Third, a few patients with benign GGNs in this study still had no definite features because of small sample sizes. Further studies with larger sample sizes are required.

Conclusions

In conclusion, benign GGNs have some common CT features. Nodules with isolated, blurred internal high-attenuation zones connecting to the blood vessels and peripheral ill-defined GGO (Type I), or nodules abutting but not surrounding blood vessels (Type II) are likely to be benign and might be resolved during follow-up. Therefore, when GGNs with these certain characteristics are detected, follow-up should be strongly considered in their clinical management, which may be helpful to reduce the unnecessary operations of non-cancerous GGNs.

Abbreviations

GGN: ground-glass nodule; GGO; ground-glass opacity; MPR, Multiplanar reconstruction; WBC: white blood cell.

Declarations

Ethics approval and consent to participate: This retrospective study was approved by the medical ethical committee of the First Affiliated Hospital of Chongqing Medical University and the requirement for informed consent was waived.

Consent for publication: Not applicable.

Availability of data and material The datasets generated and/or analyzed during the current study are available from the corresponding author on reasonable request.

Competing interests: The authors have no competing interests to disclose.

Funding: This work was supported by the National Natural Science Foundation of China (81601545) and Chongqing Health and Family Planning Commission Foundation (2016MSXM018) of China.

Authors' contributions WJL and FJL contributed to the conceptualization, writing-original draft preparation, writing-review and editing, supervision, and visualization. FJL contributed to the writing-review, editing and supervision. YWT and BJF contributed to the statistical analysis. All authors have approved the final version of the work.

Acknowledgments Not applicable.

References

1. Mao R, She Y, Zhu E, Chen D, Dai C, Wu C, et al. Proposal for Restaging of Invasive Lung Adenocarcinoma Manifesting as Pure Ground Glass Opacity. Ann Thorac Surg. 2019;107(5):1523–

31. doi:10.1016/j.athoracsur.2018.11.039.

2. She Y, Zhao L, Dai C, Ren Y, Zha J, Xie H, et al. Preoperative nomogram for identifying invasive pulmonary adenocarcinoma in patients with pure ground-glass nodule: A multi-institutional study. Oncotarget. 2017;8(10):17229–38. doi:10.18632/oncotarget.11236.
3. Henschke CI, Yankelevitz DF, Mirtcheva R, McGuinness G, McCauley D, Miettinen OS, et al. CT screening for lung cancer: frequency and significance of part-solid and nonsolid nodules. Am J Roentgenol. 2002;178(5):1053–7. doi:10.2214/ajr.178.5.1781053.
4. Kim HY, Shim YM, Lee KS, Han J, Yi CA, Kim YK. Persistent pulmonary nodular ground-glass opacity at thin-section CT: histopathologic comparisons. Radiology. 2007;245(1):267–75. doi:10.1148/radiol.2451061682.
5. Kim H, Park CM, Koh JM, Lee SM, Goo JM. Pulmonary subsolid nodules: what radiologists need to know about the imaging features and management strategy. Diagn Interv Radiol. 2014;20(1):47–57. doi:10.5152/dir.2013.13223.
6. Tsutani Y, Miyata Y, Yamanaka T, Nakayama H, Okumura S, Adachi S, et al. Solid tumors versus mixed tumors with a ground-glass opacity component in patients with clinical stage IA lung adenocarcinoma: Prognostic comparison using high-resolution computed tomography findings. J Thorac Cardiovasc Surg. 2013;146(1):17–23. doi:10.1016/j.jtcvs.2012.11.019.
7. Park CM, Goo JM, Lee HJ, Lee CH, Chun EJ, Im JG. Nodular ground-glass opacity at thin-section CT: histologic correlation and evaluation of change at follow-up. Radiographics. 2007;27(2):391–408. doi:10.1148/rg.272065061.
8. Park CM, Goo JM, Lee HJ, Lee CH, Chung DH, Chun EJ, et al. Focal interstitial fibrosis manifesting as nodular ground-glass opacity: thin-section CT findings. Eur Radiol. 2007;17(9):2325–31. doi:10.1007/s00330-007-0596-z.
9. Austin JH, Garg K, Aberle D, Yankelevitz D, Kuriyama K, Lee HJ, et al. Radiologic implications of the 2011 classification of adenocarcinoma of the lung. Radiology. 2013;266(1):62–71. doi:10.1148/radiol.12120240.
10. Oda S, Awai K, Liu D, Nakaura T, Yanaga Y, Nomori H, et al. Ground-glass opacities on thin-section helical CT: differentiation between bronchioloalveolar carcinoma and atypical adenomatous hyperplasia. AJR Am J Roentgenol. 2008;190(5):1363–8. doi:10.2214/AJR.07.3101.
11. Lee HJ, Goo JM, Lee CH, Park CM, Kim KG, Park EA, et al. Predictive CT findings of malignancy in ground glass nodules on thin-section chest CT: the effects on radiologist performance. Eur Radiol. 2009;19(3):552–60. doi:10.1007/s00330-008-1188-2.
12. Takahashi S, Tanaka N, Okimoto T, Tanaka T, Ueda K, Matsumoto T, et al. Long term follow-up for small pure ground-glass nodules: implications of determining an optimum follow-up period and high-resolution CT findings to predict the growth of nodules. Jpn J Radiol. 2012;30(3):206–17. doi:10.1007/s11604-011-0033-8.
13. Fan L, Liu SY, Li QC, Yu H, Xiao XS. Multidetector CT features of pulmonary focal ground-glass pacity: differences between benign and malignant. Br J Radiol. 2012;85(1015):897–904.

doi:10.1259/bjr/33150223.

14. Felix L, Serra-Tosio G, Lantuejoul S, Timsit JF, Moro-Sibilot D, Brambilla C, et al. CT characteristics of resolving ground-glass opacities in a lung cancer screening programme. Eur J Radiol. 2011;77(3):410–6. doi:10.1016/j.ejrad.2009.09.008.
15. Li F, Sone S, Abe H, Macmahon H, Doi K. Malignant versus Benign Nodules at CT Screening for Lung Cancer: Comparison of Thin-Section CT Findings. Radiology. 2004;233(3):793–8. doi:10.1148/radiol.2333031018.
16. Nambu A, Araki T, Taguchi Y, Ozawa K, Miyata K, Miyazawa M, et al. Focal area of ground-glass opacity and ground-glass opacity predominance on thin-section CT: Discrimination between neoplastic and non-neoplastic lesions. Clin Radiol. 2005;60(9):1006–17. doi:10.1016/j.crad.2005.06.006.
17. Yang W, Sun Y, Fang W, Qian F, Ye J, Chen Q, et al. High-resolution Computed Tomography Features Distinguishing Benign and Malignant Lesions Manifesting as Persistent Solitary Subsolid Nodules. Clin Lung Cancer. 2018;19(1):e75–83. doi:10.1016/j.cllc.2017.05.023.
18. Oh JY, Kwon SY, Yoon HI, Lee SM, Yim JJ, Lee JH, et al. Clinical significance of a solitary ground-glass opacity (GGO) lesion of the lung detected by chest CT. Lung Cancer. 2007;55(1):67–73. doi:10.1016/j.lungcan.2006.09.009.
19. Lee SM, Park CM, Goo JM, Lee CH, Lee HJ, Kim KG, et al. Transient Part-Solid Nodules Detected at Screening Thin-Section CT for Lung Cancer: Comparison with Persistent Part-Solid Nodules. Radiology. 2010;255(1):242–51. doi:10.1148/radiol.09090547.
20. Zhao F, Yan SX, Wang GF. CT features of focal organizing pneumonia: An analysis of consecutive histopathologically confirmed 45 cases. Eur J Radiol. 2014;83(1):73–8. doi:10.1016/j.ejrad.2013.04.017.
21. de Hoop B, Gietema H, van de Vorst S, Murphy K, van Klaveren RJ, Prokop M. Pulmonary ground-glass nodules: increase in mass as an early indicator of growth. Radiology. 2010;255(1):199–206. doi:10.1148/radiol.09090571.
22. Gao F, Li M, Ge X, Zheng X, Ren Q, Chen Y, et al. Multi-detector spiral CT study of the relationships between pulmonary ground-glass nodules and blood vessels. Eur Radiol. 2013;23(12):3271–7. doi:10.1007/s00330-013-2954-3.
23. Lv YG, Bao JH, Xu DU, Yan QH, Li YJ, Yuan DL, et al. Characteristic analysis of pulmonary ground-glass lesions with the help of 64-slice CT technology. Eur Rev Med Pharmacol Sci. 2017;21(14):3212–7. PMID: 28770963.
24. Naidich DP, Bankier AA, MacMahon H, Schaefer-Prokop CM, Pistolesi M, Goo JM, et al. Recommendations for the management of subsolid pulmonary nodules detected at CT: a statement from the Fleischner Society. Radiology. 2013;266(1):304–17. doi:10.1148/radiol.12120628.
25. Baldwin DR, Callister ME, Guideline Development Group. The British Thoracic Society guidelines on the investigation and management of pulmonary nodules. Thorax. 2015;70(8):794–8. doi:10.1136/thoraxjnl-2015-207168.

26. Hiramatsu M, Inagaki T, Inagaki T, Matsui Y, Satoh Y, Okumura S, et al. Pulmonary ground-glass opacity (GGO) lesions—large size and a history of lung cancer are risk factors for growth. J Thorac Oncol. 2008;3(11):1245–50. doi:10.1097/JTO.0b013e318189f526.
27. Libby DM, Wu N, Lee IJ, Farooqi A, Smith JP, Pasmantier MW, et al. CT screening for lung cancer: the value of short-term CT follow-up. Chest. 2006;129(4):1039–42. doi:10.1378/chest.129.4.1039.

Figures

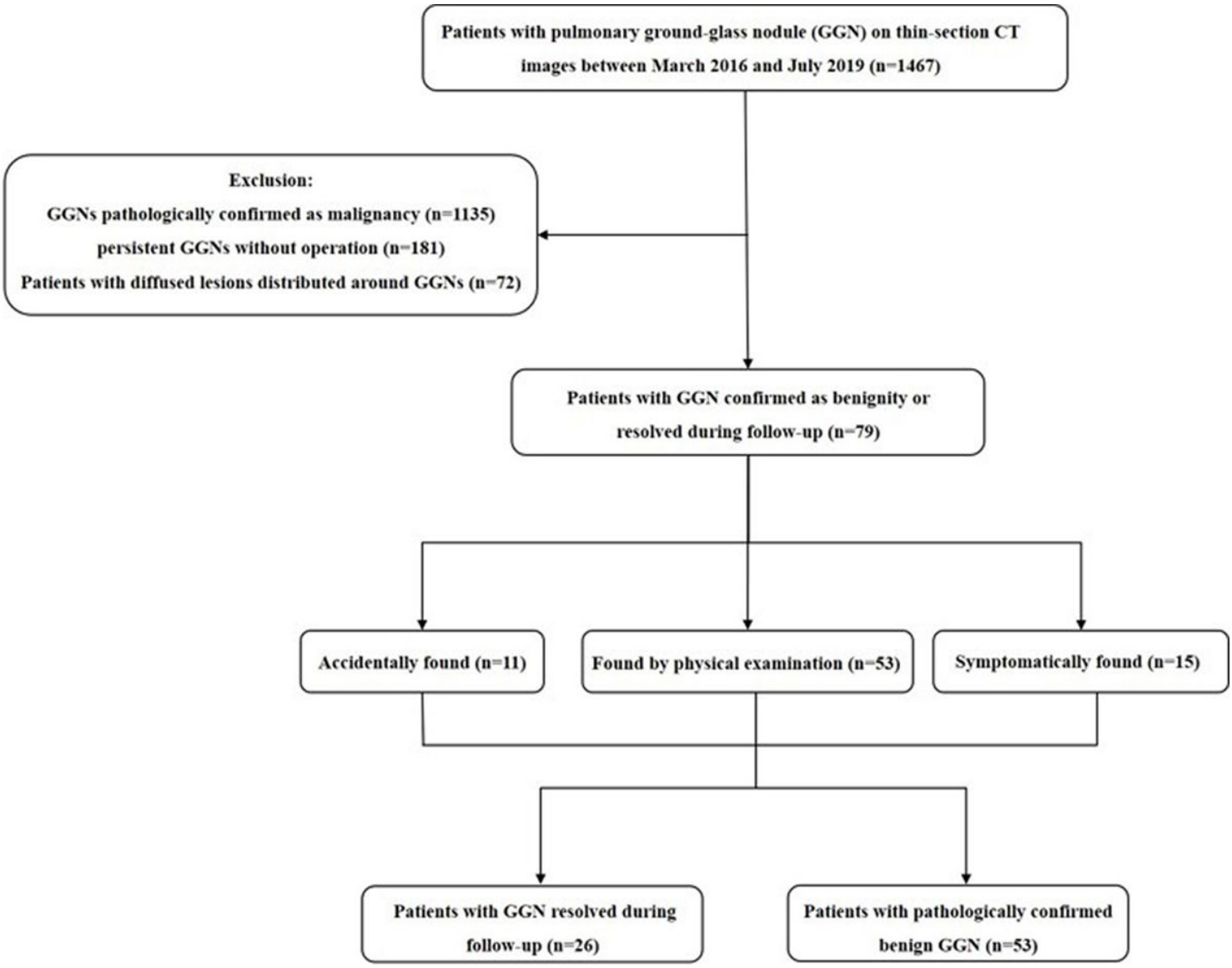

Figure 1

. Flowchart of study population. GGN = ground-glass nodule.

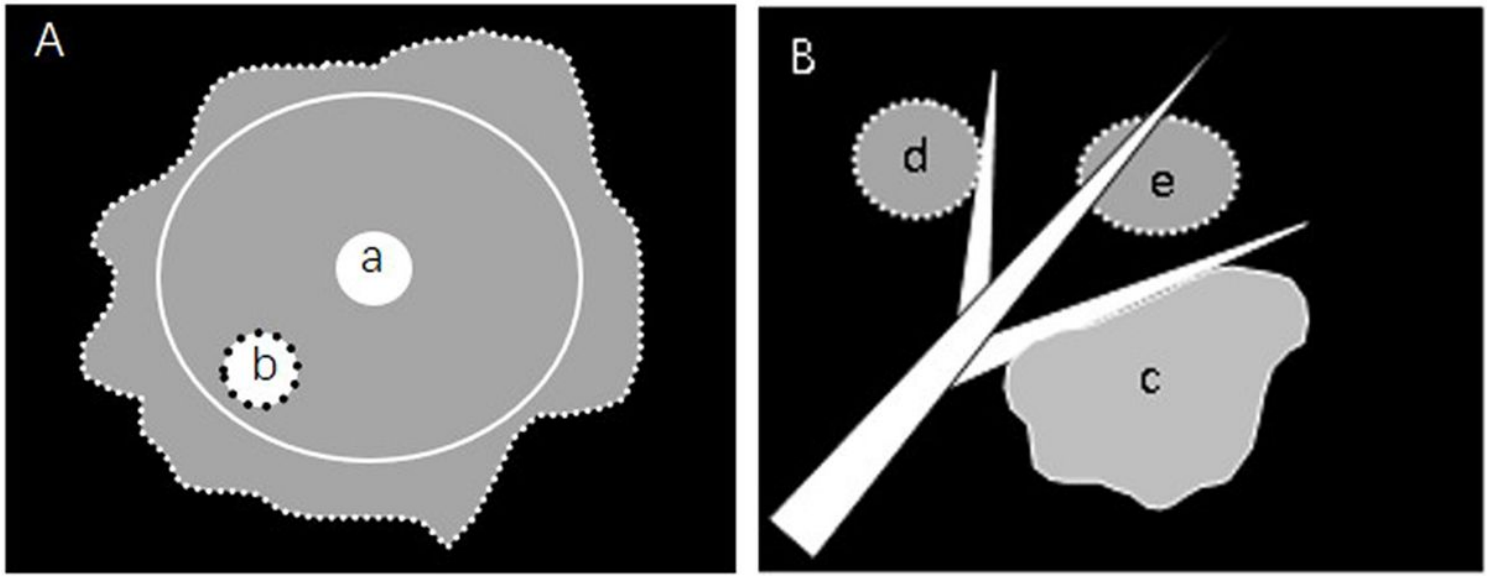

Figure 2

CT manifestations of type I and II GGNs. A, Type I GGN is defined as a regular (marked by white solid line) or irregular (marked by white dotted line) GGO containing an internal centric (a) or eccentric (b) high-attenuation zone. B. Type II GGN is defined when one nodule edge abuts an adjacent blood vessel, and the length of this edge close to the vessel is more than or equal to two thirds of the nodule's long diameter on the same section (c). The GGNs locally cling to the blood vessels (d) or surrounding the blood vessels (e) could not be seen as type II lesions.

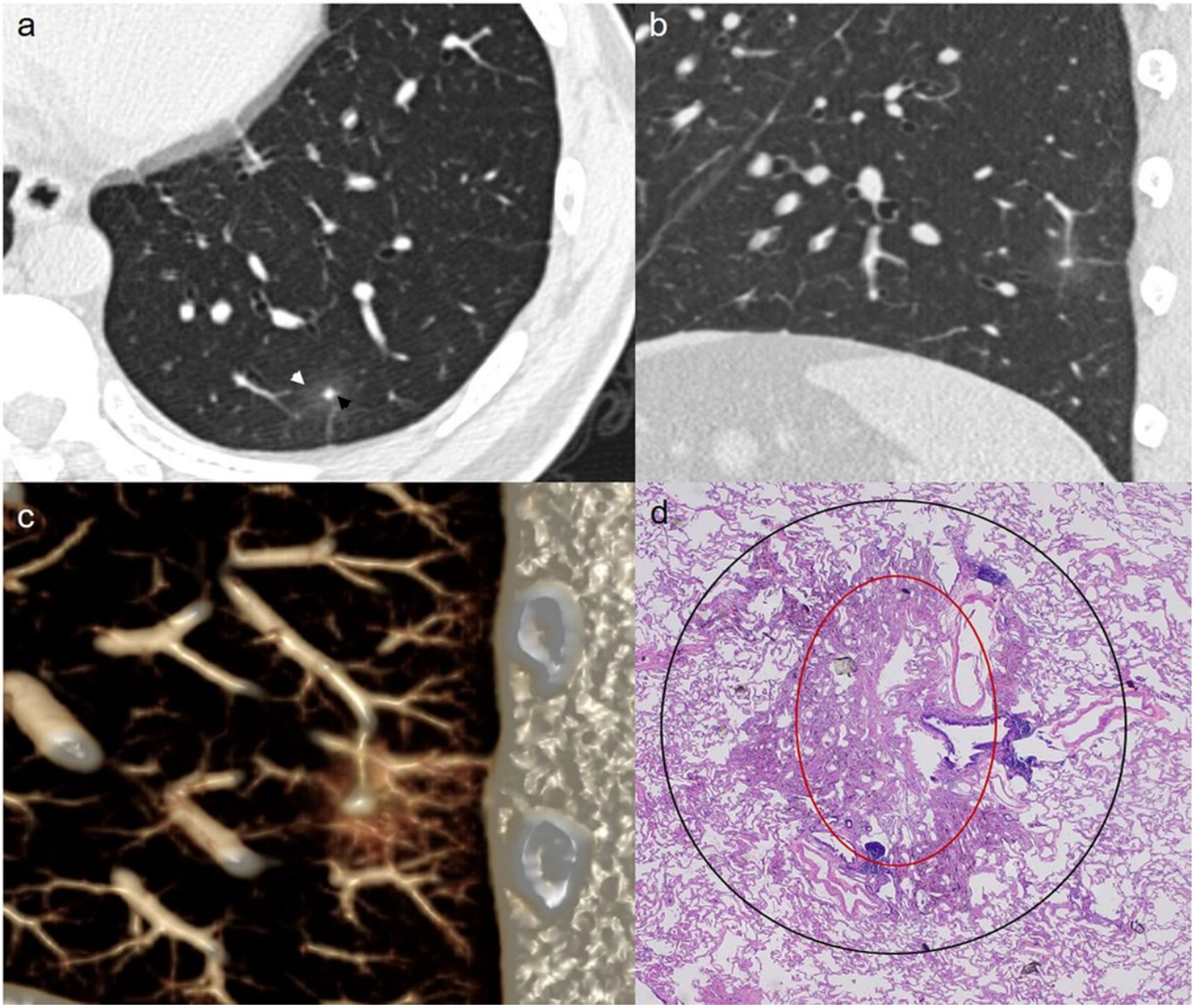

Figure 3

A patient with a type I GGN confirmed by surgical operation. Axial CT image (a) shows a 16.6 mm round mixed GGN located in the left lower lobe, the internal high-attenuation zone (black arrow) is centric, round, and blurred, and the peripheral GGO (white arrow) is ill-defined. Sagittal CT image (b) and VR image (c) confirm that the internal high-attenuation zone is connected to an adjacent blood vessel. Histopathologic analysis (d) reveals thickened alveolar walls with inflammatory cells, fibrous tissue and exudation in high-attenuation zone and a small amount of inflammatory cell infiltration in the peripheral GGO zone.

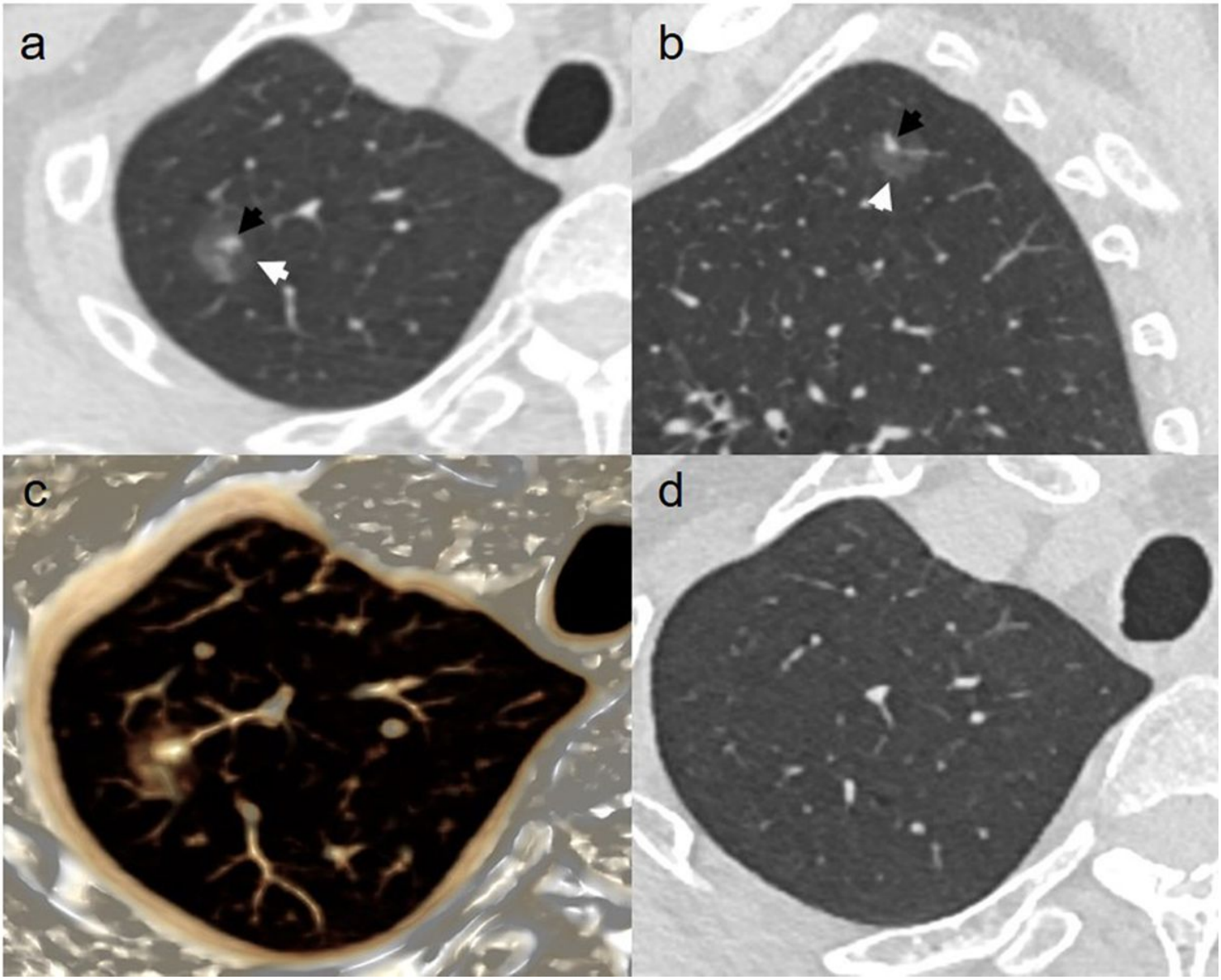

Figure 4

A patient with a transient type I GGN. He had blood eosinophilia (eosinophil count, 620/ul). Axial (a) and sagittal (b) CT images show a 13.7 mm oval mixed GGN located in the right upper lobe, the internal high-attenuation (black arrow) zone is eccentric, irregular, and blurred, and the peripheral GGO (white arrow) is partly ill-defined. VR image (c) confirm that the internal high-attenuation zone is connected to an adjacent blood vessel. At follow-up CT (d) obtained 2.5 months later, the GGN has disappeared.

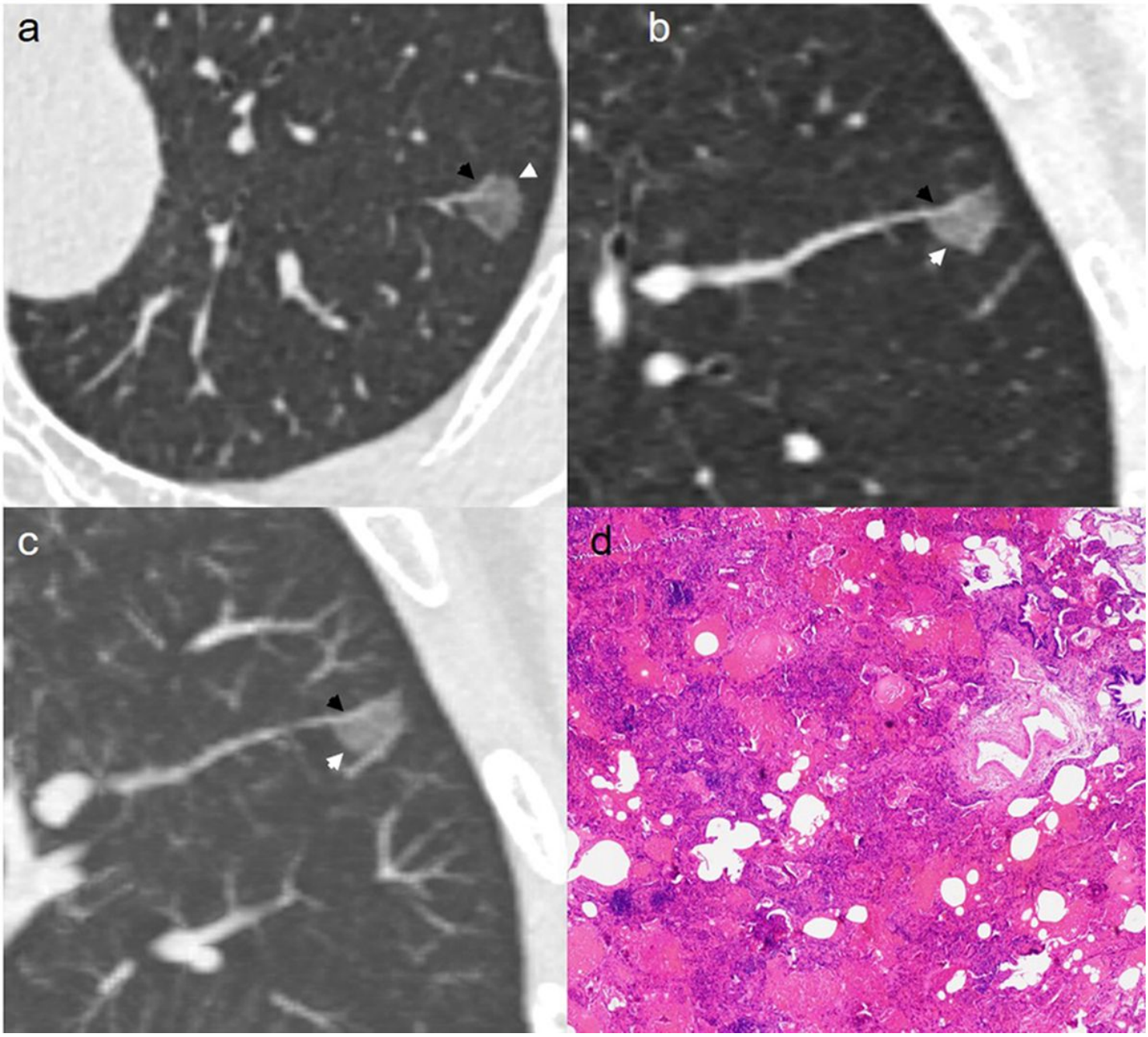

Figure 5

A patient with a type II GGN confirmed by surgical operation. Axial CT image (a) shows a 9 mm round well-defined GGN (white arrow) with slightly coarse margin located in the left upper lobe. A blood vessel (black arrow) is close to the edge of this lesion. MPR (b) and MIP (c) images confirm that one edge of this nodule (white arrow) widely abuts the upper blood vessel (black arrow). Histopathologic analysis (d) reveals focal interstitial fibrosis with inflammatory cell infiltration. (GGN = ground-glass nodule; MPR = multiplanar reconstruction; MIP = maximum intensity project)

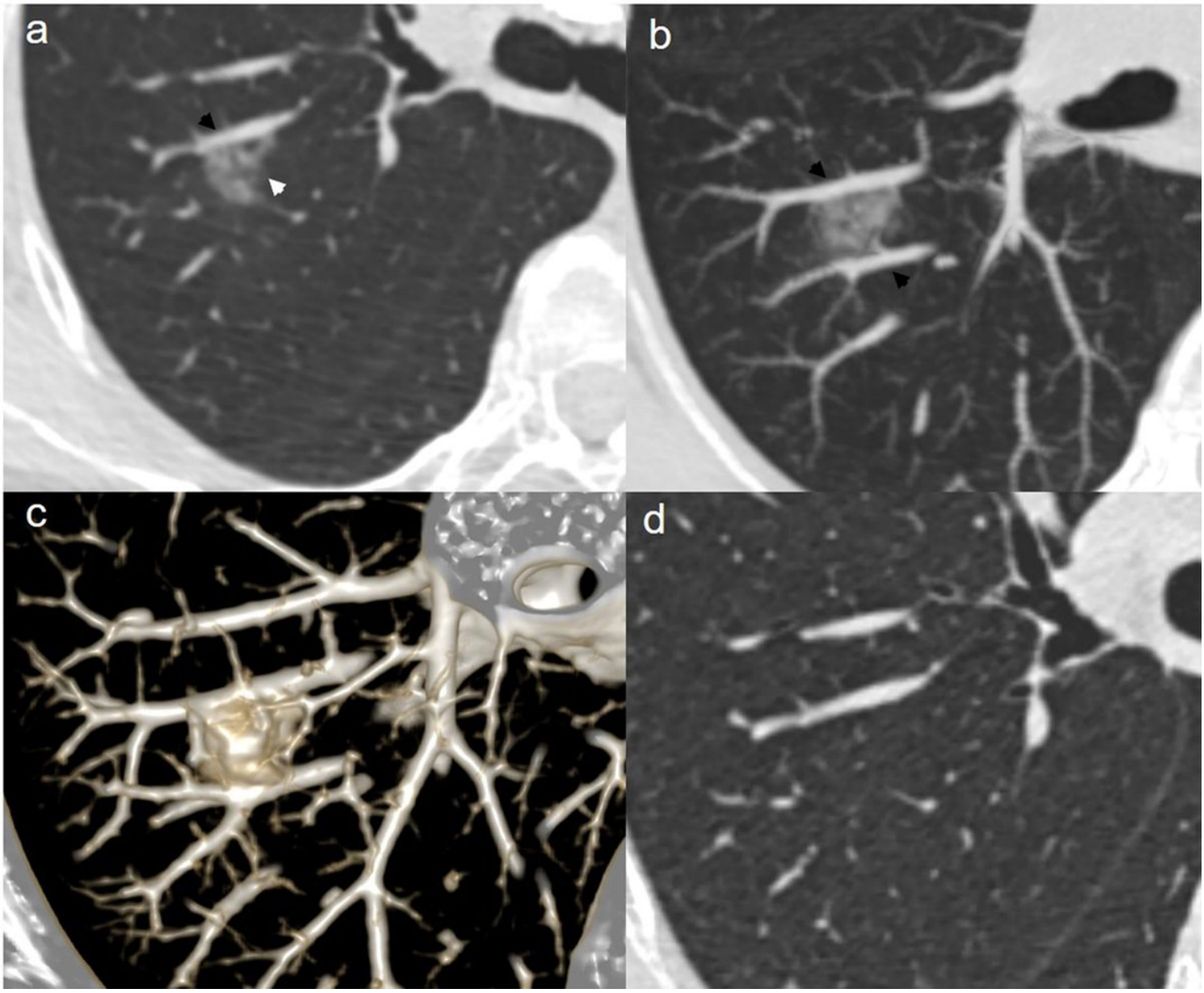

Figure 6

A patient with a type II GGN confirmed by surgical operation. Axial CT image (a) shows a 9 mm round well-defined GGN (white arrow) with slightly coarse margin located in the left upper lobe. A blood vessel (black arrow) is close to the edge of this lesion. MPR (b) and MIP (c) images confirm that one edge of this nodule (white arrow) widely abuts the upper blood vessel (black arrow). Histopathologic analysis (d) reveals focal interstitial fibrosis with inflammatory cell infiltration. (GGN = ground-glass nodule; MPR = multiplanar reconstruction; MIP = maximum intensity project)